The Astrophysical Journal, 658:557–568, 2007 March 20

DISCOVERY OF A HIGH PROPER MOTION L DWARF BINARY: 2MASS J15200224−4422419AB

Adam J. Burgasser,[1,2] Dagny L. Looper,[2,3] J. Davy Kirkpatrick,[4] and Michael C. Liu[3]

Received 2006 September 6; accepted 2006 November 21

ABSTRACT

We report the discovery of the wide L1.5+L4.5 binary 2MASS J15200224−4422419AB, identified during spectroscopic follow-up of high proper motion sources selected from the Two Micron All Sky Survey. This source was independently identified by Kendall et al. in the SuperCOSMOS Sky Survey. Resolved *JHK* photometry and low-resolution near-infrared spectroscopy demonstrate that this system is composed of two well-separated ($1.174'' \pm 0.016''$) L dwarfs. Component classifications are derived using both spectral ratios and comparison to the near-infrared spectra of previously classified field L dwarfs. Physical association for the pair is deduced from the large common proper motion of the components ($\mu = 0.73'' \pm 0.03''$ yr^{-1}) and their similar spectrophotometric distances (19 ± 2 pc). The projected separation of the binary, 22 ± 2 AU, is consistent with maximum separation/total system-mass trends for very low mass binaries. The 2MASS J1520−4422 system exhibits both large tangential (66 ± 7 km s^{-1}) and radial velocities (-70 ± 18 km s^{-1}), and its motion in the local standard of rest suggests that it is an old member of the Galactic disk population. This system joins a growing list of well-separated (>0.5″), very low mass binaries, and is an excellent target for resolved optical spectroscopy to constrain its age, as well as trace activity/rotation trends near the hydrogen-burning limit.

Subject headings: binaries: visual — stars: individual (2MASS J15200224−4422419) — stars: low-mass, brown dwarfs

Online material: color figures

1. INTRODUCTION

Multiple stellar systems are important laboratories for a wide range of astrophysical phenomena, from the formation and evolution of planetary systems to the distribution of dark matter in the Galaxy. Stellar multiples drive novae outbursts in cataclysmic variable systems, are useful distance ladders for star clusters in the local Group, and provide one of the few direct means of measuring stellar mass. The production of multiples is inherent to the star formation process itself, and the aggregate properties of multiple systems in a given population can provide insight into the genesis of that population.

Multiples are of particular importance in the study of very low mass (VLM; $M \leq 0.1\ M_\odot$) stars and brown dwarfs. Several of the first brown dwarfs identified were found as companions to nearby stars (Becklin & Zuckerman 1988; Nakajima et al. 1995; Rebolo et al. 1998), and >75 binaries composed entirely of VLM dwarfs are now known (Burgasser et al. 2006b, and references therein).[5] The salient properties of these systems—their small separations, high mass ratios, and low frequency—have been used as empirical tests of brown dwarf formation theories (Reid et al. 2001b; Burgasser et al. 2003, 2006b; Close et al. 2003; Bouy et al. 2004; Siegler et al. 2005). Astrometric monitoring of resolved doubles has provided direct measures of mass for a few VLM binaries (Lane et al. 2001; Bouy et al. 2004; Brandner et al. 2004; Zapatero Osorio et al. 2004), while the recently identified eclipsing binary 2MASS J0535218−054608AB has enabled the first radius measurement in the substellar regime (Stassun et al. 2006). Coupled with independent age determinations, these observations also constrain brown dwarf evolutionary theories (Zapatero Osorio et al. 2004; Stassun et al. 2006). Multiplicity provides explanations for other observed phenomena, such as peculiar features in individual brown dwarf spectra (Cruz et al. 2004; McGovern 2005; Burgasser et al. 2005b) and unusual photometric trends across the transition between L-type and T-type brown dwarfs (Burgasser et al. 2006; Liu et al. 2006).

Despite their fecundity, only a limited number of VLM binaries have resolved spectroscopic measurements.[6] Such observations provide detailed information on the components of these systems, and can clarify empirical trends as a function of spectral type, temperature, or mass by eliminating the variables of age and composition (assuming coeval formation). One regime in which such conditions can be exploited is the transition between the M and L dwarf spectral classes (Kirkpatrick 2005). Occurring at an effective temperature $T_{\rm eff} \approx 2300$ K (Golimowski et al. 2004; Vrba et al. 2004), this transition is characterized by the formation of photospheric condensates that dominate the near-infrared spectra of L dwarfs (Tsuji et al. 1996; Jones & Tsuji 1997; Burrows & Sharp 1999; Allard et al. 2001; Ackerman & Marley 2001), a rapid decline in the frequency and strength of Hα emission, related to the presence of a hot chromosphere (Gizis et al. 2000; Mohanty et al. 2002; West et al. 2004), and an increase in mean rotational velocities, possibly related to a change in angular momentum loss mechanisms or age effects (Mohanty & Basri 2003).

[1] Massachusetts Institute of Technology, Kavli Institute for Astrophysics and Space Research, Cambridge, MA; ajb@mit.edu.

[2] Visiting Astronomer at the Infrared Telescope Facility, which is operated by the University of Hawaii under Cooperative Agreement NCC 5-538 with the National Aeronautics and Space Administration, Office of Space Science, Planetary Astronomy Program.

[3] Institute for Astronomy, University of Hawaii, Honolulu, HI.

[4] Infrared Processing and Analysis Center, California Institute of Technology, Pasadena, CA.

[5] A current list is maintained by N. Siegler at http://paperclip.as.arizona.edu/~nsiegler/VLM_binaries.

[6] Resolved spectroscopy of VLM binaries is reported in Goto et al. (2002), Potter et al. (2002), Bouy et al. (2004), Chauvin et al. (2004), Luhman (2004), McCaughrean et al. (2004), Billéres et al. (2005), Burgasser & McElwain (2006), Close et al. (2007), Jayawardhana & Ivanov (2006), Kendall et al. (2007), McElwain & Burgasser (2006), Martín et al. (2006), and Mohanty et al. (2006).

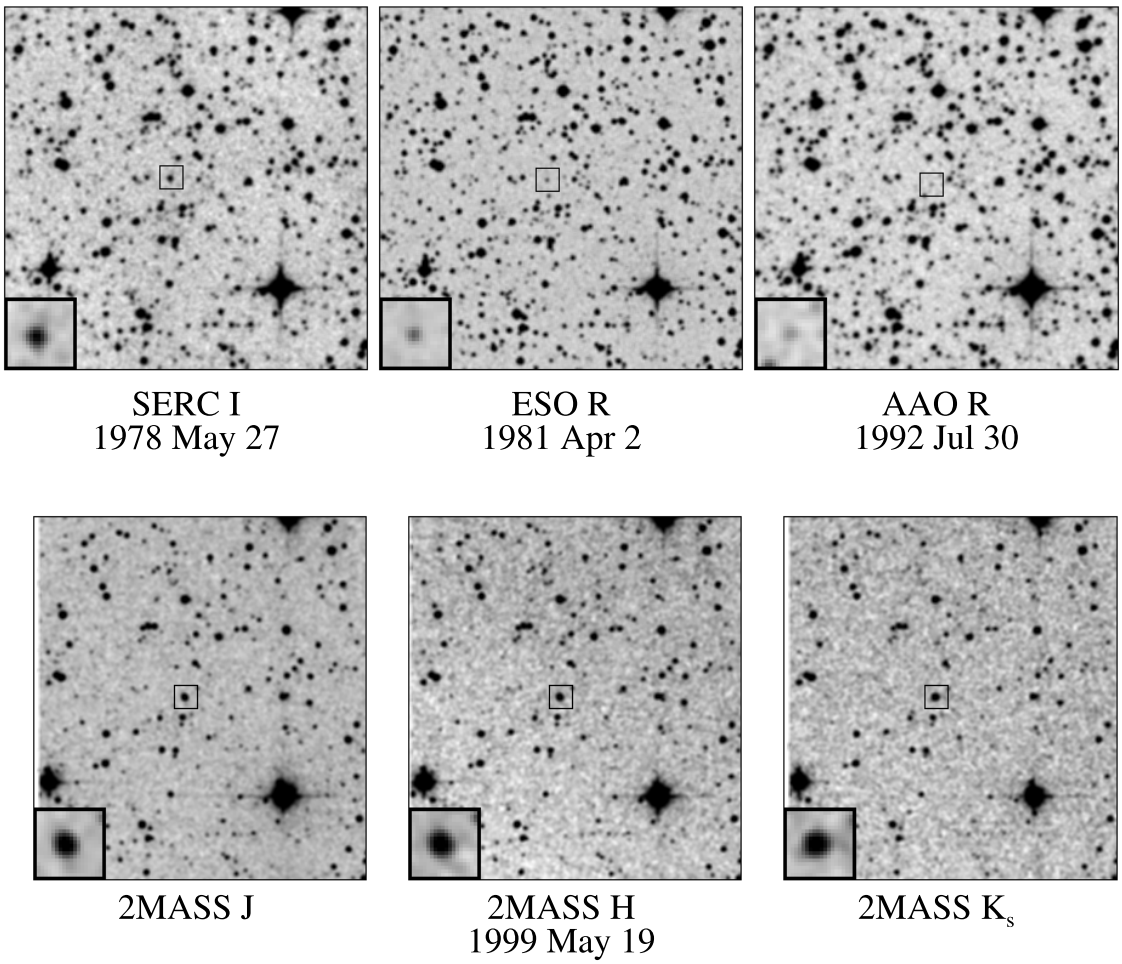

FIG. 1.—Field images of 2MASS J15200224−4422419 from SERC I_N (*top left*), ESO R (*top middle*), and AAO R (*top right*) photographic plates, and from 2MASS (*bottom*). All images are scaled to the same resolution and oriented with north up and east to the left. Photographic plate images are 5′ on a side. Inset boxes $20'' \times 20''$ in size indicate the position of the source after correcting for its motion, and are expanded in the lower left corner of each image.

In addition, late M and early L spectral types encompass the transition between hydrogen-burning stars and brown dwarfs, depending on the age of the population (Chabrier et al. 2000; Burrows et al. 2001).

Our group is currently conducting a near-infrared proper motion survey using multi-epoch data from the Two Micron All Sky Survey (2MASS; Skrutskie et al. 2006). The goal of this program is to identify late-type, nearby, and/or high-velocity sources that may have been missed by existing photographic plate proper motion surveys or near-infrared searches based solely on color-selection criteria. Details on the survey will be presented in a forthcoming publication (J. D. Kirkpatrick et al., in preparation). Here we report the identification of a well-resolved L dwarf binary system, 2MASS J15200224−4422419 (hereafter 2MASS J1520−4422). This source has been independently identified by Kendall et al. (2007) by combining 2MASS and SuperCOSMOS Sky Survey (SSS; Hambly et al. 2001a, 2001b, 2001c) catalog data. Our initial identification of this source is described in § 2. Its recognition as a binary in follow-up imaging observations and measurements of separation, position angle, and flux ratios are described in § 3. In § 4 we present near-infrared spectroscopic observations obtained with the SpeX spectrograph (Rayner et al. 2003) mounted on the 3 m NASA Infrared Telescope Facility (IRTF). These include resolved low-resolution spectra that identify the components as L dwarfs, and composite moderate-resolution data that reveal detailed spectral features similar to previously studied L dwarfs. Analysis of our observations is provided in § 5, including spectral classification of the components, kinematics of the system, and additional binary parameters. We discuss 2MASS J1520−4422 in the context of other well-resolved binaries in § 6, and motivate future spectroscopic investigations to apply the "binary Li test." Results are summarized in § 7.

2. IDENTIFICATION OF 2MASS J1520−4422

2MASS J1520−4422 was identified as a relatively bright ($J = 13.23 \pm 0.03$) and red ($J - K_s = 1.33 \pm 0.04$) unresolved source, imaged twice by 2MASS on 1999 May 19 and 2001 February 10 (UT). The difference in the astrometry of this source between the two imaging epochs implies a proper motion $\mu = 0.72'' \pm 0.12''$ yr^{-1} at a position angle $\theta = 235°$. As shown in Figure 1, counterparts of 2MASS J1520−4422 can be seen in SERC I_N (epoch 1978 May 27 UT) and ESO R (epoch 1981 April 2 UT) photographic plates, offset by $16.6''$ and $15.2''$, respectively, at the positions expected from the 2MASS proper motion. A marginal source is also present in a 1992 July 30 (UT) AAO R-band photographic plate. SSS measurements of 2MASS J1520−4422 give $I_N = 17.04$, $R_{\rm ESO} = 19.41$, and $\mu = 0.74'' \pm 0.17''$ yr^{-1}.

To obtain a more refined measure of its proper motion, we combined the SSS and 2MASS astrometry of 2MASS J1520−4422

TABLE 1
ASTROMETRY FOR 2MASS J15200224−4422419AB

Epoch (UT)	R.A.[a]	Decl.[a]	Source
1978 May 27.....	15 20 03.46	−44 22 34.1	SERC I_N (SSS)
1981 Apr 2.....	15 20 03.34	−44 22 35.6	ESO R (SSS)
1999 May 19.....	15 20 02.24	−44 22 41.9	2MASS
2001 Feb 10.....	15 20 02.14	−44 22 42.7	2MASS

NOTE.—Units of right ascension are hours, minutes, and seconds, and units of declination are degrees, arcminutes, and arcseconds.
[a] Equinox J2000.0 coordinates.

spanning 22.7 yr, as listed in Table 1. Linear fits to the right ascension and declination over this period yield $\mu_\alpha \cos\delta = -0.634'' \pm 0.013''$ yr^{-1} and $\mu_\delta = -0.367'' \pm 0.012''$ yr^{-1}, for a combined motion of $\mu = 0.73'' \pm 0.03''$ yr^{-1} at $\theta = 239.9^\circ \pm 1.0^\circ$. Note that these values do not take into consideration parallactic motion. The high proper motion of this optically faint red source made it a high-priority target for follow-up observations.

3. IMAGING OBSERVATIONS

3.1. *Data Acquisition and Reduction*

2MASS J1520−4422 was imaged again in the near-infrared on 2006 April 8 (UT) using SpeX on IRTF. Conditions during this night were poor, with patchy cirrus and clouds. Seeing was 0.8″–0.9″ at the J band. Acquisition images with the instrument's guiding camera immediately revealed two distinct sources at the position of 2MASS J1520−4422, separated by roughly 1″. After rechecking telescope focus, we obtained a series of 20 s exposures of the pair in the J, H, and K filters,[7] interspersed with images of the nearby, bright point source 2MASS J15195960−4421523 ($J = 13.20 \pm 0.03$, $J - K_s = 0.72 \pm 0.04$) as a point-spread function (PSF) calibrator. Four dithered exposures were obtained for each source and filter, for a total of 80 s integration each. We also obtained twilight and bias exposures in all three filters on 2006 April 11 (UT) during the same observing campaign for pixel response calibration.

The imaging data were cleaned using a pixel mask constructed from the bias and twilight images, then pair-wise subtracted and divided by a normalized flat-field frame constructed from the median-combined, bias-subtracted twilight observations (appropriate to the respective filter). The calibrated images were centered and co-added to produce a mosaic for each filter/pointing combination. Figure 2 displays $6'' \times 6''$ subsections of these mosaics for the target and PSF star. Two sources are clearly resolved at the position of 2MASS J1520−4422, lying along a northwest-southeast axis. The northernmost source is markedly brighter in all three bands, particularly at J and H.

3.2. *PSF Fitting*

Relative astrometry and photometry of the 2MASS J1520−4422 pair were determined using the same iterative PSF fitting algorithm described in Burgasser & McElwain (2006). For each filter, we fit centered $6'' \times 6''$ subsections of each pair-wise subtracted image of 2MASS J1520−4422 to equivalent subsections for all four PSF images, a total of 16 fits per filter. The fitting algorithm first determined an initial estimate of the peak position

[7] *JHK* filters on SpeX are based on the Mauna Kea Observatory near-infrared (MKO-NIR) filter set (Simons & Tokunaga 2002; Tokunaga et al. 2002).

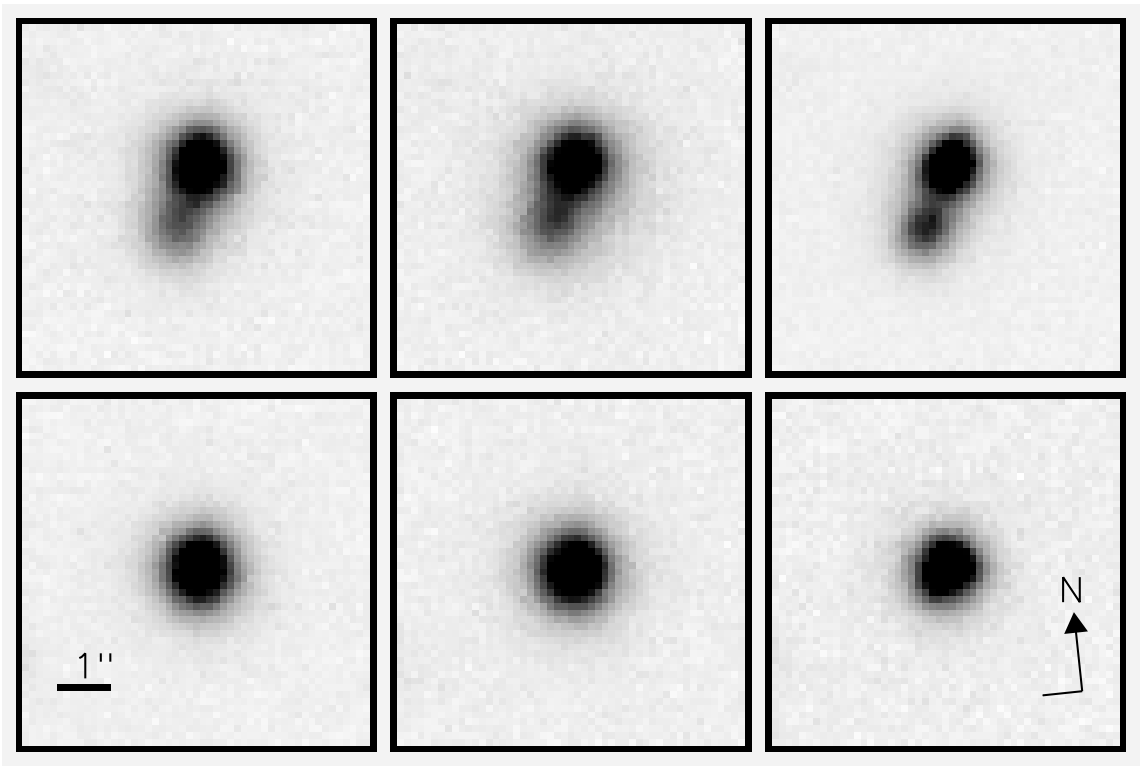

FIG. 2.—SpeX images of 2MASS J15200224−4422419AB (*top*) and the PSF calibrator 2MASS J15195960−4421523 (*bottom*) at J (*left*), H (*middle*), and K (*right*). Images are 6″ on a side. The image scale is indicated in the bottom left image, and the orientation of all six images (6.4° ± 0.3°) is indicated in the bottom right image.

TABLE 2
PROPERTIES OF THE 2MASS J15200224−4422419AB SYSTEM

Parameter	Value	Reference
α[a]	$15^h20^m02.24^s$	1
δ[a]	$-44°22'41.9''$	1
μ	$0.73'' \pm 0.03''$ yr^{-1}	1, 2, 3
θ	$239.9° \pm 1.0°$	1, 2, 3
NIR SpT	L1.5 + L4.5	3
d_{est}	19 ± 2 pc	3
ρ	$1.174'' \pm 0.016''$	3
	22 ± 2 AU	3
ϕ	$152.9° \pm 0.7°$	3
V_{tan}	66 ± 7 km s^{-1}	3
V_{rad}	-70 ± 18 km s^{-1}	3
(U, V, W)	$(50, 30, -20)$ km s^{-1}	3
R_{ESO}[b]	19.41 mag	2
I_N[b]	17.04 mag	2
J[b]	13.23 ± 0.03 mag	1
H[b]	12.36 ± 0.03 mag	1
K_s[b]	11.89 ± 0.03 mag	1
ΔJ	1.15 ± 0.08 mag	3
ΔH	0.97 ± 0.06 mag	3
ΔK	0.95 ± 0.03 mag	3
M_{tot}[c]	0.14–0.16 $M_\odot$	3, 4
Period[c]	~400 yr	3, 4

[a] Equinox J2000.0 coordinates at epoch 1999 May 19 from 2MASS.
[b] Photometry for combined (unresolved) system.
[c] Assuming an age of 1–10 Gyr.
REFERENCES.—(1) 2MASS (Skrutskie et al. 2006); (2) SSS (Hambly et al. 2001a, 2001b, 2001c); (3) This paper; (4) Burrows et al. 1997.

and fluxes of the two components, then recursively matched model images (constructed from the PSF frames) to the data. The primary pixel coordinates, secondary pixel coordinates, primary flux, and secondary flux in the model image were adjusted iteratively in steps of 0.1 pixels and 0.01 fraction flux until residuals were minimized, of order 1%–2% of the source peak flux. The mean of the flux ratios,[8] separations (ρ), and position angles (ϕ) for each filter are listed in Table 2. Uncertainties include scatter in the PSF fit measurements, and values take into account the pixel scale ($0.120'' \pm 0.002''$ pixel^{-1}) and rotator position ($6.4° \pm 0.3°$; J. Rayner 2005, private communication) of SpeX during the observations. As in Burgasser & McElwain (2006), we found no systematic offsets in our fitting results based on PSF simulations.

To determine component magnitudes, we combined our relative flux measurements with composite photometry from 2MASS. Because relative fluxes were measured using MKO-NIR filters, we first derived the filter translation factors $\delta_M = M^{2MASS} - M^{MKO}$ for each component, where $\Delta M^{2MASS} = \Delta M^{MKO} + \delta_{M,B} - \delta_{M,A}$, as described in McElwain & Burgasser (2006). These factors were calculated by convolving filter response curves (filter transmission function × optical response × telluric absorption at an air mass of 1) for 2MASS (Cohen et al. 2003; see Cutri et al. 2003, § IV.4.a) and MKO-NIR filters (S. Leggett 2004, private communication) with the individual component spectra (§ 4.1) and a spectrum of the A0 V star Vega (Hayes 1985; Mountain et al. 1985). These calculations yield $\delta_{J,B} - \delta_{J,A} = 0.018$, $\delta_{H,B} - \delta_{H,A} = -0.001$, and $\delta_{K,B} - \delta_{K,A} = -0.001$. The filter translation factors are therefore negligible, likely due to the similarity of the component spectra in the regions sampled by the *JHK* filters, and were disregarded. Component magnitudes are listed in Table 3.

[8] Note that the imaging observations were taken in nonphotometric conditions; however, we assume that the relative atmospheric transmission over the small separation of the 2MASS J1520−4422 pair was constant and that any differential atmospheric absorption has minimal effect on the relative flux within each individual filter.

3.3. *Common Proper Motion*

The high proper motion of 2MASS J1520−4422 and the brightness of its components allow us to immediately deduce common proper motion for this pair. Both components are bright enough to be detected individually by 2MASS. Since the earliest 2MASS image of this field was taken 6.89 yr prior to the SpeX observations, at least one of these sources would have moved a full $5.05''$ from the SpeX position, easily resolvable by 2MASS. Since no secondary source is seen in these earlier images (Fig. 1), implying a limiting separation of $\sim 1.5''$ (Burgasser et al. 2005a), we conclude that the two sources are comoving to within $\sim 0.2''$ yr^{-1} of motion and to within $\sim 15°$–$20°$ in position angle. These limits are sufficiently stringent that common proper motion can be confidently claimed, and we refer to this pair hereafter as 2MASS J1520−4422AB.

4. SPECTROSCOPIC OBSERVATIONS

4.1. *Prism Spectroscopy*

Resolved, low-resolution near-infrared spectral data for the 2MASS J1520−4422 components were obtained on 2006 April 8 (UT), also using SpeX. We used the $0.3''$ slit to better separate flux from each component, yielding 0.75–2.5 μm spectra with resolution $\lambda/\Delta\lambda \approx 250$ and dispersion across the chip of 20–30 Å pixel^{-1}. To obtain separate spectra for each component, we set the image rotator to 300° so that one source lay in the slit while the other source was positioned orthogonal to the slit axis and used for guiding (Fig. 3). This orientation was not aligned with the parallactic angle (~15°), and as the observations were made at fairly large air mass (2.42–2.60), differential refraction (DR) effects are expected (Filippenko 1982, see below). Six and eight exposures of 90 s each were obtained for the A and B components, respectively, both in an ABBA dither pattern. The A0 V star HD 133820 was observed immediately afterward, at a similar air mass (2.66) and with the slit aligned to the parallactic angle, for flux calibration.

TABLE 3
PROPERTIES OF THE 2MASS J15200224−4422419AB COMPONENTS

			2MASS			Estimated Mass[b]		
Component	NIR SpT	T_{eff}[a] (K)	J (mag)	H (mag)	K_s (mag)	1 Gyr ($M_\odot$)	5 Gyr ($M_\odot$)	10 Gyr ($M_\odot$)
2MASS J1520−4422A	L1.5	2200	13.55 ± 0.04	12.73 ± 0.03	12.27 ± 0.03	0.075	0.082	0.082
2MASS J1520−4422B	L4.5	1740	14.70 ± 0.07	13.70 ± 0.05	13.22 ± 0.04	0.064	0.077	0.078

[a] T_{eff} estimate from Vrba et al. (2004).
[b] Based on the solar metallicity models of Burrows et al. (1997).

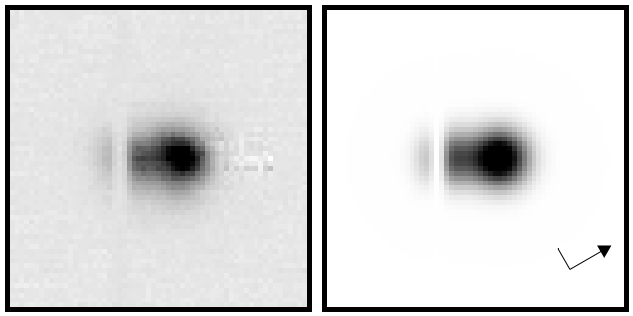

FIG. 3.—*Left*: Stacked *K*-band images of 2MASS J1520−4422 during acquisition of the fainter component. The brighter component was used for guiding, while the secondary was offset slightly from the slit center to minimize contamination. *Right*: Model of the guider image used to compute differential refraction (DR) and contamination effects. Both images are 7.2″ on a side, and orientation on the sky is indicated by the arrow.

Internal flat-field and Ar arc lamps were then observed for pixel response and wavelength calibration.

Data were reduced using the SpeXtool package, version 3.3 (Cushing et al. 2004), using standard settings. First, the images were corrected for linearity, pair-wise subtracted, and divided by the corresponding median-combined flat-field image. Spectra were optimally extracted using the default settings for aperture and background source regions, and wavelength calibration was determined from arc lamp and sky emission lines. Multiple spectral observations for each source were then median-combined after scaling the individual spectra to match the observation with the highest signal-to-noise ratio. Telluric and instrumental response corrections for the science data were determined using the method outlined in Vacca et al. (2003), with line shape kernels derived from the arc lines. Adjustments were made to the telluric spectra to compensate for differing H I line strengths in the observed A0 V spectrum and pseudovelocity shifts. Final calibration was made by multiplying the observed target spectrum by the telluric correction spectrum, which includes instrumental response correction through the ratio of the observed A0 V spectrum to a scaled, shifted, and deconvolved Kurucz[9] model spectrum of Vega.

Corrections for DR effects in the spectrum of the fainter component, in terms of both slit losses and contamination from the bright primary, were determined by simulating the light throughput for both sources as a function of wavelength. We first created a model of stacked *K*-band guiding images (acquired at one dither position during the spectral observations) using two symmetric Gaussian surfaces and a box-car slit profile. The widths of the Gaussian profiles were determined by one-dimensional Gaussian fits of image slices through the brighter component parallel to the slit axis. Note that these values are slightly larger (∼1″) than the measured seeing, due to telescope guiding jitter. We adjusted the fluxes and pixel offsets (perpendicular to the slit) of the two components in our model using an iterative algorithm similar to that used for the PSF fitting, minimizing residuals with respect to the *K*-band guider image. Figure 3 displays the best-fit model; note that the secondary was actually centered slightly off the slit. We then calculated DR pixel shifts as a function of wavelength using the formalism of Roe (2002; see also Schubert & Walterscheid 2000), assuming standard atmospheric pressure and temperature, a relative humidity of 50%, and a true zenith distance of 55.5°. The calculated shifts move both components closer to the slit center at wavelengths shorter than 2.2 μm, by as much as 1.5 pixels at 1.2 μm. Hence, slit losses are greatest at the longest wavelengths,

[9] See http://kurucz.harvard.edu/stars.html.

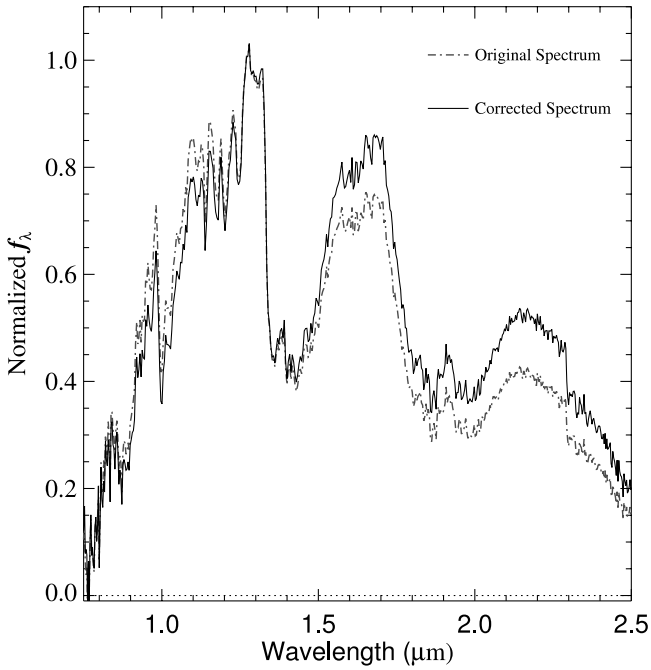

FIG. 4.—SpeX prism spectrum of 2MASS J1520−4422B before (*dash-dotted line*) and after (*solid line*) correction of differential refraction (DR) and contamination effects. Both spectra are normalized at 1.28 μm. [*See the electronic edition of the Journal for a color version of this figure*.]

while contamination from the primary is greatest at the shortest wavelengths. Both effects were calculated using our model images by shifting the centers of the Gaussian profiles in accordance with the DR shifts (keeping the seeing and relative flux ratios constant) and calculating the total light throughput for both components in the slit. We found slit losses to be roughly 20% at *K* relative to *J*, while light contamination ranged from 3% at *K* to >10% for $\lambda < 1.2$ μm.

The spectrum of 2MASS J1520−4422B was corrected for slit losses using that component's model-derived relative throughput values. Contamination from the primary was removed by subtracting a spectrum of 2MASS J1520−4422A scaled by the wavelength-dependent contribution of its light through the slit relative to the secondary from the DR model. Figure 4 shows the spectrum of 2MASS J1520−4422B before and after these effects have been accounted for. The corrected spectrum is significantly redder, as both slit losses and light contamination suppress *K*-band light from this component. Similar simulations were used to calculate DR slit losses for the spectrum of the primary, assuming it to be centered on the slit at the *K* band. These were smaller (<10% slit loss for $\lambda > 1$ μm) due to the large size of the seeing disk relative to the slit width. Light contamination from the secondary was found to be negligible.

The reduced prism spectra (including DR and contamination corrections) of the two 2MASS J1520−4422 components are shown in Figure 5. These spectra are qualitatively similar to *JH* spectra presented in Kendall et al. (2007). Both components have spectral energy distributions consistent with early-type L dwarfs, including red optical and near-infrared spectral slopes, deep H_2O absorption bands at 1.4 and 1.9 μm, strong CO absorption at 2.3 μm, FeH and CrH bands at 0.86, 0.99, 1.2, and 1.6 μm, a notable absence of TiO and VO features shortward of 1 μm, and unresolved Na I and K I atomic lines at the *J* band (Reid et al. 2001a; Testi et al. 2001; McLean et al. 2003; Nakajima et al. 2004). The 0.99 μm FeH band in 2MASS J1520−4422B is unusually strong, although this may be due to uncorrected DR effects. The stronger

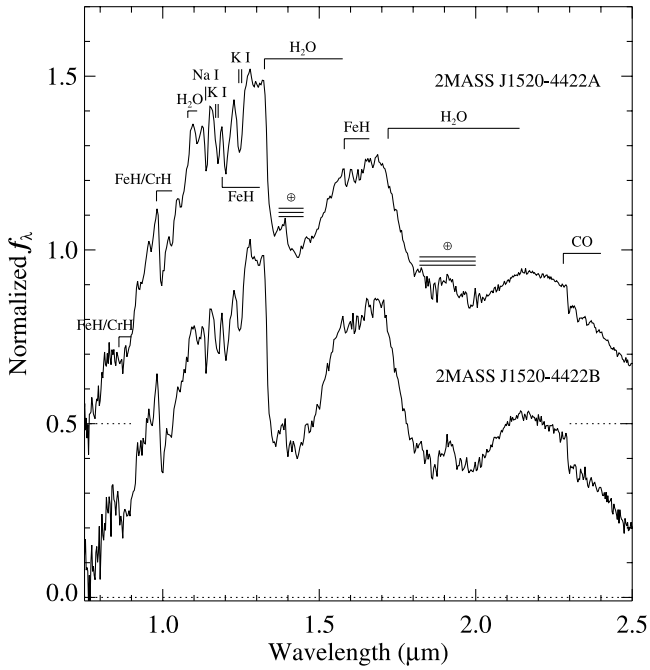

FIG. 5.—Near-infrared SpeX spectra of 2MASS J1520−4422A (*top*) and B (*bottom*). Data are normalized at 1.28 μm, with 2MASS J1520−4422A offset by a constant for clarity (*dotted lines*). Major molecular (FeH, CrH, H_2O, and CO) and atomic (Na I and K I) absorption features are labeled, as well as regions of strong telluric absorption (⊕).

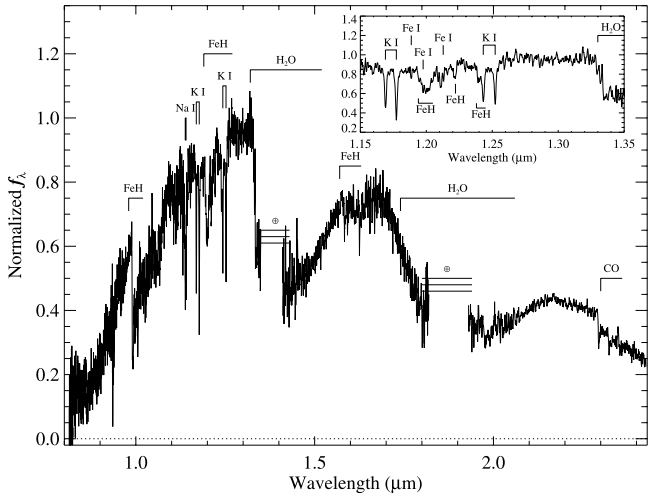

FIG. 6.—Cross-dispersed spectrum of the composite 2MASS J1520−4422 system. Data are normalized at 1.28 μm. Major molecular and atomic absorption features are indicated, as well as regions of strong telluric absorption (⊕). The inset shows a close-up view of the 1.15–1.35 μm region, hosting several K I and Fe I lines and FeH and H_2O molecular bands.

H_2O and FeH molecular bands of 2MASS J1520−4422B, and its redder near-infrared color, indicate that it is of later type than 2MASS J1520−4422A.

4.2. *Cross-dispersed Spectroscopy*

Higher resolution cross-dispersed (XD) spectra for the composite system (i.e., both sources simultaneously in the slit) were obtained on 2006 April 11 (UT). Conditions on this night were somewhat improved, with light cirrus and moderate seeing (0.8″ at the *J* band). The 0.5″ slit was used for a spectral resolution $\lambda/\Delta\lambda \approx 1200$ and dispersion across the chip of 2.7–5.3 Å pixel^{-1}. The slit was aligned to the parallactic angle, and 8 exposures (4 of 250 s, 4 of 300 s) dithered in an ABBA pattern were obtained for a total integration time of 2200 s. HD 133820 was again observed immediately after 2MASS J1520−4422 and at a similar air mass (2.75), followed by calibration lamps. As with the prism data, XD data were reduced using the SpeXtool package, following similar procedures but using a line shape kernel derived from the 1.005 μm H I Pa δ line in the A0 V calibrator spectra. After telluric and flux calibration, the five orders spanning 0.82–2.43 μm were scaled and combined using the prism spectrum of 2MASS J1520−4422A as a relative flux template.

The reduced XD spectrum for 2MASS J1520−4422 is shown in Figure 6. While these data have lower overall signal-to-noise ratio than the prism data (particularly shortward of 0.98 μm and in the telluric bands), many of the small wiggles observed in this spectrum are real, arising largely from H_2O and FeH transitions and numerous atomic metal lines. The strongest atomic features are the Na I and K I doublet lines at the *J* band, which are shown in detail in the inset of Figure 6. In addition, there are several lines from Fe I and FeH and broader FeH bands in this spectral region. CO band heads at 2.299, 2.328, 2.357, and 2.388 μm are clearly discerned, but the 2.206/2.209 μm Na I doublet is notably absent. The absence of this feature provides further evidence that 2MASS J1520−4422 is composed of L dwarfs (McLean et al. 2003; Cushing et al. 2005). Similarly, the absence of the 1.314 μm Al I line is consistent with an L spectral type, while the presence of the 1.189 μm Fe I line suggests a composite spectral type of L3 or earlier (McLean et al. 2003).

Equivalent widths (EW) of the 1.169, 1.178, and 1.253 μm K I lines and 1.189 Fe I line were measured using Gaussian fits to the line profiles and linear fits to the nearby pseudocontinuum (the 1.244 μm K I was not measured, as its blue wing is blended with an FeH band). Values of 6 ± 2, 8.3 ± 1.8, 8.0 ± 1.6, and 0.5 ± 0.2 Å, respectively, were derived and are comparable to other early-type L dwarfs (Cushing et al. 2005).

5. ANALYSIS

5.1. *Spectral Classification and Estimated Distance*

The resolved prism spectra of the 2MASS J1520−4422 components allow us to derive individual spectral types. However, while a robust classification scheme for L dwarfs exists at optical wavelengths (Kirkpatrick et al. 1999, 2000), there is as yet no well-defined scheme in the near-infrared, i.e., following the tenets of the MK Process (Morgan et al. 1943; Corbally et al. 1994). We therefore determined subtypes for these sources using a variety of spectral indices from the literature that are applicable to low-resolution near-infrared spectral data. Reid et al. (2001a) have defined several indices measuring the strengths of H_2O and CO bands, as well as color ratios, for late-type M and L dwarf spectra. They provide linear spectral type calibrations anchored to optical classifications for their H_2O-A and H_2O-B indices (sampling the 1.1 and 1.4 μm H_2O bands) and the *K*1 index of Tokunaga & Kobayashi (1999) over spectral types M8 to L6. Testi et al. (2001) defined six indices, sampling H_2O bands and color ratios for spectral data of comparable resolution to our SpeX prism observations, and provided linear calibrations for these indices over types L0 to L8. Burgasser et al. (2002) also defined H_2O band indices and color ratios, as well as CH_4 band indices, in their near-infrared classification scheme for T dwarfs; three of the H_2O indices show good correlation with M5–L7 optical spectral type, and one CH_4 index correlates with L3–T3 spectral types. Finally, Geballe et al. (2002) utilized several near-infrared indices to classify late-type M, L, and T dwarfs, two of which (H_2O 1.5 μm and CH_4 2.2 μm) are

TABLE 4
Near-infrared Spectral Classification Indices

Index	2MASS J1520−4422A		2MASS J1520−4422B		2MASS J1520−4422AB (XD)	
	Value	SpT	Value	SpT	Value	SpT
Reid et al. (2001a)						
H_2O-A	0.686	L1.5	0.597	L4	0.656	L2.5
H_2O-B	0.749	L2	0.639	L5	0.718	L3
$K1$[a]	0.178	L1	0.297	L3.5	0.219	L2
Testi et al. (2001)						
sH_2O^J	0.165	L2.5	0.259	L4	0.229	L3.5
sH_2O^{H1}	0.327	L2	0.510	L4	0.343	L2
sH_2O^{H2}	0.443	L2	0.538	L4	0.517	L4
sH_2O^K	0.197	L0.5	0.332	L4	0.255	L2
Burgasser et al. (2002)						
H_2O-A	0.878	L1.5	0.806	L5	0.835	L3.5
H_2O-B	0.857	L1.5	0.790	L5	0.836	L2.5
H_2O-C	0.868	L1	0.782	L6.5	0.861	L1.5
CH_4-C	0.991	...	0.954	L4.5	0.990	...
Geballe et al. (2002)						
H_2O 1.5 μm	1.333	L1.5	1.592	L5.5	1.407	L2
CH_4 2.2 μm	0.973	...[b]	1.013	L5	0.975	...[b]
Mean NIR SpT	L1.5 ± 0.6		L4.5 ± 0.8		L2.5 ± 0.8	

[a] Index defined in Tokunaga & Kobayashi (1999).
[b] Index/SpT relation not defined for SpT < L3 (Burgasser et al. 2002; Geballe et al. 2002).

applicable in the L dwarf regime (for spectral types L0–L9 and L3–L9, respectively). Unlike the other near-infrared schemes, Geballe et al. (2002) tie spectral types to their indices with predetermined numerical ranges set by measurements for a large sample of VLM dwarf spectra.

Table 4 lists the values and associated spectral types of these indices for each component spectrum prism of 2MASS J1520−4422, as well as the composite XD spectrum. Note that we have not included color indices from Testi et al. (2001) and Burgasser et al. (2002), due to possible residual DR effects. There is fairly consistent agreement in the derived spectral types between these schemes, likely due to the similarity in features used to define the indices (primarily H_2O bands). Mean subtypes for all indices are L1.5 and L4.5 for 2MASS J1520−4422A and B, with scatter of 0.6 and 0.8 subtypes, respectively. This is consistent with the types derived by Kendall et al. (2007), L2 and L4, within the stated uncertainties. The XD spectrum is classified L2.5 ± 0.8, as expected for contributions from both components to the combined light spectrum.

To confirm these classifications, we compared the prism spectra to an array of equivalent data for previously classified field L dwarfs with similar optical and/or near-infrared subtypes, as shown in Figure 7. The spectrum of 2MASS J1520−4422A is nearly identical to that of 2MASS J20575409−0252302, classified L1.5 from both optical (Cruz et al. 2003) and near-infrared (Kendall et al. 2004) data, and appears to be intermediate between those of optically classified L1 (2MASS J14392836+1929149; Kirkpatrick et al. 1999 spectral standard) and L2 (SSSPM J0829−1309; Scholz & Meusinger 2002) comparison sources. Similarly, the spectrum of 2MASS J1520−4422B shows remarkable agreement with that of the optically classified L4 2MASS J11040127+1959217 (Cruz et al. 2003), and less agreement with those of optically classified L3 (SDSS J202820.32+005226.5; Hawley et al. 2002) and L5 dwarfs (GJ 1001BC; Goldman et al. 1999). These comparisons would appear to verify the index-based classifications from Table 4, and indicate that the DR and light contamination corrections applied to the spectrum of 2MASS J1520−4422B were accurate.

The agreement of the near-infrared spectra of 2MASS J1520−4422A and B with those of optically classified sources suggests that the derived subtypes could be adopted as their optical classifications. However, a number of studies (Stephens 2003; Knapp et al. 2004; Kirkpatrick 2005) have found that optical and near-infrared spectral types cannot be assumed to be identical for mid- and late-type L dwarfs, due to the complexity of their atmospheres. Figure 8 illustrates that this is an issue even among early-type L dwarfs, comparing SpeX prism data for three optically classified L2 dwarfs—SSSPM J0829−1309, Kelu 1 (Ruiz et al. 1997), and SIPS J0921−2104 (Deacon et al. 2005)—to that of 2MASS J1520−4422A. Despite their equivalent optical classifications, these three sources have very different near-infrared spectra. Both SSSPM J0829−1309 and Kelu 1 appear to have redder 1–2.5 μm spectra than 2MASS J1520−4422A, while SIPS J0921−2104 is bluer. SSSPM J0829−1309 has weaker 1.4 and 1.7 μm H_2O absorption, while these same bands are markedly deeper in the spectrum of SIPS J0921−2104. The spectral indices used above yield mean near-infrared subtypes of L1, L2.5, and L4 for SSSPM J0829−1309, Kelu 1, and SIPS J0921−2104, respectively (see also Knapp et al. [2004] and Lodieu et al. [2005] regarding the near-infrared spectrum of Kelu 1). Such classification disagreements have been attributed to a variety of causes, including variations in photospheric dust content (Stephens 2001, 2003), unresolved multiplicity (Burgasser et al. 2005b; Liu & Leggett 2005), and gravity effects (McGovern et al. 2004; Kirkpatrick

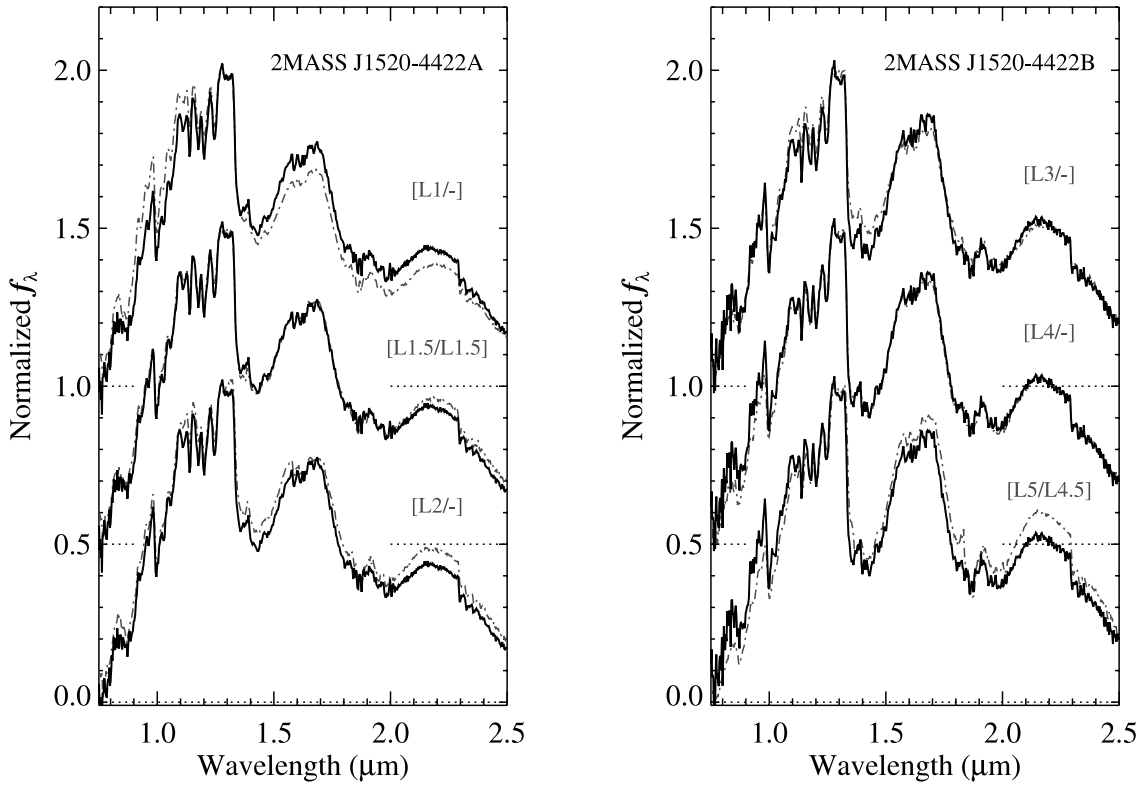

FIG. 7.—Comparison of the near-infrared spectra of 2MASS J1520−4422A and B (*solid lines in left and right panels, respectively*) to equivalent data (*dash-dotted lines*) for the spectral comparison stars. In the left panel we compare 2MASS J1520−4422A to 2MASS J14392836+1929149 (L1 optical classification), 2MASS J20575409−0252302 (L1.5 optical and near-infrared classification), and SSSPM J0829−1309 (L2 optical classification). In the right panel we compare 2MASS J1520−4422B to SDSS J202820.32+005226.5 (L3 optical classification), 2MASS J11040127+1959217 (L4 optical classification), and GJ 1001BC (L5 optical classification, L4.5 near-infrared classification). All spectra have been normalized at 1.28 μm and offset by constants (*dotted lines*). [*See the electronic edition of the Journal for a color version of this figure.*]

et al. 2006). These complexities emphasize the need for a robust, independent, and multidimensional near-infrared classification scheme for L dwarfs.

Assuming that the derived near-infrared spectral types for 2MASS J1520−4422A and B are at least suitable proxies for their optical classifications, spectrophotometric distance estimates for each component were computed using measured photometry and absolute 2MASS magnitude/spectral type relations from Dahn et al. (2002), Cruz et al. (2003), Tinney et al. (2003), and Vrba et al. (2004). These yield mean distances of 19.1 ± 0.8 and 19.1 ± 0.7 pc for 2MASS J1520−4422A and B, respectively, assuming no uncertainty in the spectral types. The agreement in the estimated distances for both components and their common proper motion are consistent with these two sources being gravitationally bound. We adopt a mean distance of $d_{\rm est} = 19 \pm 2$ pc, which includes a 0.5 subtype uncertainty in the classifications.

5.2. *Radial Velocity and Kinematics*

The large proper motion of 2MASS J1520−4422 and its estimated distance imply a large tangential motion, $V_{\rm tan} = 4.74 \mu d_{\rm est} = 66 \pm 7$ km s^{-1}. This is on the high end of the L dwarf $V_{\rm tan}$ distribution of Vrba et al. (2004), in which only $3/33 = 9^{+8}_{-3}$% of the sources examined have $V_{\rm tan} > 60$ km s^{-1}. Similarly, only 13^{+6}_{-3}% of late-type M and L dwarfs in the sample of Gizis et al. (2000) have $V_{\rm tan} > 60$ km s^{-1}. These studies suggest that 2MASS J1520−4422 may be an unusually high velocity system.

To determine its three-dimensional space motion, we used the XD spectrum to measure a systemic radial velocity ($V_{\rm rad}$). Despite the coarse velocity resolution of these data ($\Delta V \approx 250$ km s^{-1}), a relatively accurate determination of $V_{\rm rad}$ can be obtained through cross-correlation techniques. We compared the spectrum of 2MASS J1520−4422 to equivalent SpeX XD data from Cushing et al. (2005) for four early/mid-type L dwarfs with measured radial velocities (Bailer-Jones 2004): 2MASS J11463449+2230527 (L3; 21 ± 2 km s^{-1}), 2MASS J14392836+1929149 (L1; -26.3 ± 0.5 km s^{-1}), 2MASS J15074769−1627386 (L5; -39.3 ± 1.5 km s^{-1}), and 2MASS J22244381−0158521 (L4.5; -37 ± 3 km s^{-1}). The wavelength scale for the 2MASS J1520−4422 data was shifted by velocities ranging over −300 to 300 km s^{-1} in steps of 1 km s^{-1}. Then, for each shifted spectrum, the cross-correlation[10] was computed against each of the comparison spectra in three wave bands with strong features: the 1.16–1.26 μm region, hosting numerous K I, Fe I, and FeH absorptions (see inset of Fig. 6), the 1.32–1.34 μm region, spanning the 1.33 μm H_2O band head, and the 2.290–2.295 μm region, spanning the 2.292 μm CO band head. After correcting for the radial velocities of the comparison sources, we derived a mean $V_{\rm rad} = -60 \pm 12$ km s^{-1} for 2MASS J1520−4422, where the uncertainty is the scatter of the 12 cross-correlation measurements. As a secondary check, we measured the central wavelengths of the well-resolved 1.169, 1.177, 1.244, and 1.253 μm K I lines, using Gaussian fits to the line cores and vacuum wavelengths as listed in the Kurucz Atomic Line Database[11] (Kurucz & Bell 1995). These

[10] We computed $C(V) \propto \int_{\lambda_1}^{\lambda_2} [f_\lambda^T(V) - \bar{f}_\lambda^T](f_\lambda^C - \bar{f}_\lambda^C)\, d\lambda$, where $f_\lambda^T(V)$ is the spectrum of 2MASS J1520−4422 shifted to velocity V, f_λ^C is the spectrum of the comparison source, and $\bar{f}_\lambda$ is the mean flux over the spectral band spanning λ_1 to λ_2. The radial velocity of 2MASS J1520−4422 was determined as $V_{\rm rad} = V_{\rm max} - V_C$, where $V_{\rm max}$ is the velocity that maximizes $C(V)$ and V_C is the known radial velocity of the comparison source.

[11] Obtained through the online database search form created by C. Heise and maintained by P. Smith; see http://cfa-www.harvard.edu/amdata/ampdata/kurucz23/sekur.html.

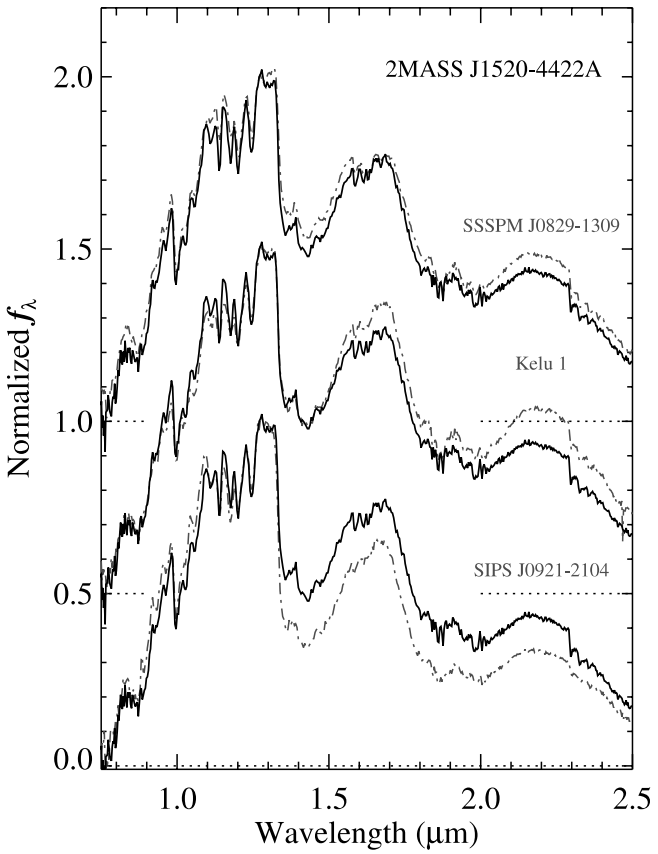

FIG. 8.—Comparison of the near-infrared spectra of 2MASS J1520−4422A (*solid lines*) to equivalent data (*dash-dotted lines*) for three optically classified L2 dwarfs: SSSPM J0829−1309, Kelu 1, and SIPS J0921−2104. All spectra have been normalized at 1.28 μm and offset by constants (*dotted lines*). [*See the electronic edition of the Journal for a color version of this figure.*]

four lines yield a mean $V_{\rm rad} = -79 \pm 24$ km s^{-1}, where the uncertainty includes systematic errors as determined from similar measurements for the four L dwarf comparison spectra used above. These two measures are consistent, and we adopt a weighted average of $V_{\rm rad} = -70 \pm 18$ km s^{-1}. Note that corrections for Earth's motion in the solar frame of reference have not been included in this value, as these corrections are significantly smaller than our estimated uncertainty.

The total space velocity of 2MASS J1520−4422 is quite high, nearly 100 km s^{-1} relative to the Sun. Combining position, proper motion, and radial velocity measurements with our estimates for the distance of 2MASS J1520−4422 yields local standard-of-rest (LSR) velocity components of $(U, V, W) \approx (50, 30, -20)$ km s^{-1}, where we have assumed $(U, V, W)_\odot = (10, 5, 7)$ km s^{-1} (Dehnen & Binney 1998). These values lie just outside of the 1 σ velocity dispersion sphere of local disk M dwarfs [$(\sigma_U, \sigma_V, \sigma_W) \approx (40, 28, 19)$ km s^{-1}, centered at $(-13, -23, -7)$ km s^{-1}; Hawley et al. 1996], suggesting old disk kinematics, but not necessarily membership in the thick disk or halo populations. The absence of any distinct low-metallicity features in the near-infrared spectra of the 2MASS J1520−4422 components that characterize L subdwarfs (Burgasser 2004) also indicates that this system is likely an old member of the Galactic disk population.

5.3. *Additional Properties of the 2MASS J1520−4422 Binary*

As early/mid-type L dwarfs, the components of 2MASS J1520−4422 are likely to have masses close to or below the hydrogen-burning minimum mass, $M \approx 0.075\ M_\odot$ (Chabrier et al. 2000; Burrows et al. 2001). However, because brown dwarfs cool over time, their $T_{\rm eff}$ and spectral types are a function of both mass and age, which are difficult to disentangle for individual field objects. In Table 3, we list estimated masses for 2MASS J1520−4422A and B for ages of 1, 5, and 10 Gyr, assuming $T_{\rm eff}$ of 2200 and 1740 K, respectively (appropriate for L1.5 and L4.5 dwarfs; Vrba et al. 2004), and the evolutionary models of Burrows et al. (1997). The kinematics of this system suggest an age older than 1 Gyr, implying masses of $\gtrsim$0.075 and $\gtrsim$0.064 $M_\odot$ for the two components, respectively. Hence, it is likely that 2MASS J1520−4422A is a low-mass star, while 2MASS J1520−4422B is either a low-mass star or a massive brown dwarf.

Our spectrophotometric distance estimate of 2MASS J1520−4422 implies a projected separation of $\rho = 22 \pm 2$ AU, which is relatively wide for a VLM binary. Indeed, Burgasser et al. (2006b) have found that 93% of known VLM binaries have $\rho < 20$ AU. However, "wide" VLM binaries such as 2MASS J1520−4422 do not violate the maximum separation/total system-mass trend of Burgasser et al. (2003), $\rho_{\rm max} = 1400 M_{\rm tot}^2$ AU, which appears to be appropriate for nearly all known binaries with $M_{\rm tot} \lesssim 0.3\ M_\odot$. These are to be distinguished from a few "ultrawide" (separations >200 AU) and/or weakly-bound ($V_{\rm esc} < 3.8$ km s^{-1}; Close et al. 2003) VLM binaries now known (Chauvin et al. 2004, 2005; Luhman 2004; Billéres et al. 2005; Close et al. 2007; Jayawardhana & Ivanov 2006), whose origin and stability remain controversial (Mugrauer & Neuhäuser 2005) and a challenge for VLM dwarf formation models (Reipurth & Clarke 2001; Bate et al. 2003). Nevertheless, 2MASS J1520−4422 is sufficiently wide that its estimated orbital period ($\sim$400 yr) is far too long to be useful for dynamical mass measurements in the near future.

6. DISCUSSION

2MASS J1520−4422 joins a growing list of VLM binaries that are sufficiently well separated to allow resolved photometric and spectroscopic studies from moderate-sized ground-based telescopes (such as IRTF) without the need for adaptive optics corrections. Table 5 lists the 16 known VLM binaries with angular separations greater than 0.5″ that fall into this category; all are resolvable from the ground at optical and near-infrared wavelengths during conditions of excellent seeing (indeed, most have been discovered and/or observed entirely with ground-based facilities). These systems are also among the most interesting VLM sources currently under investigation. Epsilon Indi Bab (Scholz et al. 2003; McCaughrean et al. 2004) is composed of the two brown dwarfs nearest to the Sun that are currently known, followed closely by the secondary of SCR 1845-6537AB (Hambly et al. 2004; Biller et al. 2006). The secondary of the 2MASS J12073347−3932540AB system, a member of the nearby $\sim$8 Myr TW Hydrae association (Gizis 2002), has an estimated mass in the planetary-mass regime ($\sim$5 Jupiter masses; Chauvin et al. 2004), and both components may harbor circumstellar accretion disks (Mohanty et al. 2003, 2006; Gizis et al. 2005). Oph 11AB (2MASS J16222521−2405139; Allers et al. 2006) is an even younger and wider ($\sim$240 AU) VLM binary whose components have masses nearly in the planetary-mass regime (Close et al. 2007; Jayawardhana & Ivanov 2006; Allers et al. 2007). 2MASS J23310161−0406193AB, ϵ Indi Bab, and Gliese 337CD are all members of higher order multiples, widely separated from more massive primaries (Gizis et al. 2000; Scholz et al. 2003; Burgasser et al. 2005a). DENIS J020529.0−115925AB may itself be a triplet of brown dwarfs (Bouy et al. 2005).

TABLE 5
VLM Binaries Wider than 0.5″

Name	ρ (arcsec)	d (pc)	R[a] (mag)	J[a] (mag)	ΔJ (mag)	SpT	References
DENIS J020529.0−115925AB[bc]	0.51	12	...	14.59	0.0	L5 + L7	1, 2, 3, 4
2MASS J04291842−3123568AB	0.53	∼11	16.2	10.89	1.2	M7.5 + [L1][d]	5, 6, 7
Gliese 337CD	0.53	21	...	15.51	0.3	L8 + [T:][d]	8, 9
2MASS J23310161−0406193AB	0.57	∼26	18.9	12.94	2.8	M8 + [L7][d]	4, 10, 11, 12
2MASS J09153413+0422045AB	0.73	∼15	...	14.55	0.1	L7 + [L7][d]	7
ϵ Indi Bab	0.73	3.6	20.8	12.29	0.9	T1 + T6	13, 14
2MASS J12073347−3932540AB	0.78	∼53	19.3	13.00	7.0	M8.5 + L:	15, 16, 17, 18, 19
2MASS J17072343−0558249AB	1.01	∼15	18.9	12.05	1.3	M9 + L3	7, 15, 20
DENIS J220002.0−303832.9AB	1.09	∼35	19.2	13.44	0.3	M9 + L0	21, 22
2MASS J15200224−4422419 AB	1.17	∼19	19.4	13.23	1.2	L1.5 + L4.5	23, 24
SCR 1845-6537AB	1.17	3.9	16.3	9.54	3.7	M8.5 + [T5.5][d]	25, 26, 27, 28
2MASS J11011926−7732383AB[c]	1.44	∼170	19.4	13.10	0.9	M7 + M8	29
2MASS J16233609−2402209AB[e]	1.70	∼125	17.4	11.53	0.7	[M5:][d] + [M5:][d]	30, 31
2MASS J16222521−2405139AB[f]	1.94	∼125	19.4	14.47	0.8	M9 + M9.5	30, 31, 32, 33
DENIS J055146.0−443412.2AB	2.20	∼100	...	15.79	0.6	M8.5 + L0	34

[a] R and J photometry for combined system from SSS and 2MASS, respectively; see also associated references.
[b] Possible triple system (Bouy et al. 2005).
[c] Resolved optical spectroscopy has been obtained for this system.
[d] Spectral type based on resolved photometry; resolved spectroscopy has not yet been reported for this source.
[e] aka Oph 16 (Allers et al. 2006).
[f] aka Oph 11 (Allers et al. 2006).

References.—(1) Delfosse et al. 1997; (2) Koerner et al. 1999; (3) Leggett et al. 2001; (4) Bouy et al. 2003; (5) Cruz et al. 2003; (6) Siegler et al. 2005; (7) Reid et al. 2006; (8) Wilson et al. 2001; (9) Burgasser et al. 2005a; (10) Gizis et al. 2000; (11) Gizis et al. 2003; (12) Close et al. 2003; (13) Scholz et al. 2003; (14) McCaughrean et al. 2004; (15) Gizis 2002; (16) Chauvin et al. 2004; (17) Chauvin et al. 2005; (18) Mamajek 2005; (19) Mohanty et al. 2006; (20) McElwain & Burgasser 2006; (21) Kendall et al. 2004; (22) Burgasser & McElwain 2006; (23) This paper; (24) Kendall et al. 2007; (25) Hambly et al. 2004; (26) Henry et al. 2004; (27) Biller et al. 2006; (28) Henry et al. 2006; (29) Luhman 2004; (30) Allers et al. 2006; (31) Close et al. 2007; (32) Jayawardhana & Ivanov 2006; (33) Allers et al. 2007; (34) Billéres et al. 2005.

While resolved near-infrared spectroscopy exists for over half of the systems listed in Table 5, only three[12] (DENIS J020529.0−115925AB, Martín et al. 2006; 2MASS J11011926−7732383AB, Luhman 2004; and Oph 11AB, Jayawardhana & Ivanov 2006) have resolved optical spectroscopy reported to date. Such observations are of particular importance for M dwarf/L dwarf binaries due to the presence of the 6563 Å Hα line, as discussed above, and the 6708 Å Li I line. The latter is a powerful indicator of mass and age for M dwarf/L dwarf field binaries, as recently pointed out by Liu & Leggett (2005). This species is depleted in the atmospheres of brown dwarfs and low-mass stars more massive than $\sim$0.065 $M_{\odot}$, due to fusion reactions in their cores (Rebolo et al. 1992). Hence, the detection of this line in the spectrum of a brown dwarf sets an upper limit for its mass and a corresponding upper limit on its age for a given $T_{\rm eff}$ and assumed evolutionary model. For a binary system composed of two coeval brown dwarfs, Li I absorption may be present in one, both, or neither component, and any of these three cases can set different constraints on the age of the system. In the case of 2MASS J1520−4422AB, if the 6708 Å Li I line is present in the spectra of both components, then the evolutionary models of Burrows et al. (1997) predict a system age of $\lesssim$600 Myr. If Li I is absent in both component spectra, then the system is $\gtrsim$1 Gyr old, consistent with its kinematics. The most interesting case is if Li I is present only in the spectrum of the secondary, as this would provide a tight constraint on the age of the system ($\sim$0.6–1 Gyr). While this "binary Li test" has been indirectly used for sources with composite optical spectroscopy (Burgasser et al. 2005b; Liu & Leggett 2005; McElwain & Burgasser 2006), the wide separation of 2MASS J1520−4422 makes it an excellent target for the first unambiguous application of this technique.

[12] Martín et al. (2006) report resolved optical spectroscopy for 9 VLM binaries based on *Hubble Space Telescope* observations, 8 of which have separations less than 0.5″. Note that these data had insufficient resolution and signal-to-noise ratio to measure Li I EW $\leq$5 Å.

7. SUMMARY

We have identified a well-resolved L1.5+L4.5 binary, 2MASS J1520−4422. This source was found by us as a high proper motion source ($\mu = 0.73'' \pm 0.03''$ yr^{-1}) in the 2MASS point source catalog, and concurrently by Kendall et al. (2007) in the SuperCOSMOS Sky Survey catalog. The apparent separation ($\rho = 1.174'' \pm 0.016''$) and estimated distance of this system (19 ± 2 pc) imply a wide projected separation (22 ± 2 AU) that is nevertheless consistent with the maximum separation/total mass relation of Burgasser et al. (2003). The 2MASS J1520−4422 system exhibits a large space velocity relative to the Sun ($V_{\rm tan} = 66 \pm 7$ km s^{-1}, $V_{\rm rad} = -70 \pm 18$ km s^{-1}), and its kinematics are consistent with an old Galactic disk dwarf system. As a source at the boundary of the hydrogen-burning mass limit, and with components spanning the early/mid-type L dwarf regime, 2MASS J1520−4422 is a prime target for resolved photometric and spectroscopic investigations of magnetic activity, dust evolution and variability, and rotational velocity trends, and a test case for the binary Li test.

The authors would like to thank telescope operator Eric Volquardsen, instrument specialist John Rayner, and Alan Tokunaga for their assistance and hospitality during the observations. A. J. B. acknowledges useful discussions with Subhanjoy Mohanty during the preparation of the manuscript and helpful comments from our referee, Herve Bouy. This publication makes use of data from the Two Micron All Sky Survey, which is a joint project of the University of Massachusetts and the Infrared Processing and Analysis Center, and funded by the National

Aeronautics and Space Administration and the National Science Foundation. 2MASS data were obtained from the NASA/IPAC Infrared Science Archive, which is operated by the Jet Propulsion Laboratory, California Institute of Technology, under contract with the National Aeronautics and Space Administration. This program has benefitted from the M, L, and T dwarf compendium housed at DwarfArchives.org and maintained by Chris Gelino, Davy Kirkpatrick, and Adam Burgasser, and the VLM Binary Archive maintained by N. Siegler at http://paperclip.as.arizona.edu/~nsiegler/VLM_binaries. The authors wish to recognize and acknowledge the very significant cultural role and reverence that the summit of Mauna Kea has always had within the indigenous Hawaiian community. We are most fortunate to have the opportunity to conduct observations from this mountain.

Facilities: IRTF(SpeX)

REFERENCES

Ackerman, A. S., & Marley, M. S. 2001, ApJ, 556, 872
Allard, F., Hauschildt, P. H., Alexander, D. R., Tamanai, A., & Schweitzer, A. 2001, ApJ, 556, 357
Allers, K. N., Kessler-Silacci, J. E., Cieza, L. A., & Jaffe, D. T. 2006, ApJ, 644, 364
Allers, K. N., et al. 2007, ApJ, 657, 511
Bailer-Jones, C. A. L. 2004, A&A, 419, 703
Bate, M. R., Bonnell, I. A., & Bromm, V. 2003, MNRAS, 339, 577
Becklin, E. E., & Zuckerman, B. 1988, Nature, 336, 656
Biller, B. A., Kasper, M., Close, L. M., Brandner, W., & Kellner, S. 2006, ApJ, 641, L141
Billéres, M., Delfosse, X., Beuzit, J.-L., Forveille, T., Marchal, L., & Martín, E. L. 2005, A&A, 440, L55
Bouy, H., Brandner, W., Martín, E. L., Delfosse, X., Allard, F., Baraffe, I., Forveille, T., & Demarco, R. 2004, A&A, 424, 213
Bouy, H., Brandner, W., Martín, E. L., Delfosse, X., Allard, F., & Basri, G. 2003, AJ, 126, 1526
Bouy, H., Martín, E. L., Brandner, W., & Bouvier, J. 2005, AJ, 129, 511
Brandner, W., Martín, E. L., Bouy, H., Köhler, R., Delfosse, X., Basri, G., & Andersen, M. 2004, A&A, 428, 205
Burgasser, A. J. 2004, ApJ, 614, L73
Burgasser, A. J., Kirkpatrick, J. D., Cruz, K. L., Reid, I. N., Leggett, S. K., Liebert, J., Burrows, A., & Brown, M. E. 2006, ApJS, 166, 585
Burgasser, A. J., Kirkpatrick, J. D., & Lowrance, P. J. 2005a, AJ, 129, 2849
Burgasser, A. J., Kirkpatrick, J. D., Reid, I. N., Brown, M. E., Miskey, C. L., & Gizis, J. E. 2003, ApJ, 586, 512
Burgasser, A. J., & McElwain, M. W. 2006, AJ, 131, 1007
Burgasser, A. J., Reid, I. N., Leggett, S. J., Kirkpatrick, J. D., Liebert, J., & Burrows, A. 2005b, ApJ, 634, L177
Burgasser, A. J., Reid, I. N., Siegler, N., Close, L. M., Allen, P., Lowrance, P. J., & Gizis, J. E. 2007, in Planets and Protostars V, ed. B. Reipurth, D. Jewitt, & K. Keil (Tucson: Univ. Arizona Press), 427
Burgasser, A. J., et al. 2002, ApJ, 564, 421
Burrows, A., Hubbard, W. B., Lunine, J. I., & Liebert, J. 2001, Rev. Mod. Phys., 73, 719
Burrows, A., & Sharp, C. M. 1999, ApJ, 512, 843
Burrows, A., et al. 1997, ApJ, 491, 856
Chabrier, G., Baraffe, I., Allard, F., & Hauschildt, P. 2000, ApJ, 542, 464
Chauvin, G., Lagrange, A.-M., Dumas, C., Zuckerman, B., Mouillet, D., Song, I., Beuzit, J.-L., & Lowrance, P. 2004, A&A, 425, L29
———. 2005, A&A, 438, L25
Close, L. M., Siegler, N., Freed, M., & Biller, B. 2003, ApJ, 587, 407
Close, L. M., et al. 2007, ApJ, submitted (astro-ph/0608574)
Cohen, M., Wheaton, W. A., & Megeath, S. T. 2003, AJ, 126, 1090
Corbally, C. J., Gray, R. O., & Garrison, R. F., ed. 1994, ASP Conf. Ser. 60, The MK Process at 50 Years: A Powerful Tool for Astrophysical Insight (San Francisco: ASP)
Cruz, K. L., Burgasser, A. J., Reid, I. N., & Liebert, J. 2004, ApJ, 604, L61
Cruz, K. L., Reid, I. N., Liebert, J., Kirkpatrick, J. D., & Lowrance, P. J. 2003, AJ, 126, 2421
Cushing, M. C., Rayner, J. T., & Vacca, W. D. 2005, ApJ, 623, 1115
Cushing, M. C., Vacca, W. D., & Rayner, J. T. 2004, PASP, 116, 362
Cutri, R. M., et al. 2003, Explanatory Supplement to the 2MASS All Sky Data Release (Pasadena: IPAC), http://www.ipac.caltech.edu/2mass/releases/allsky/doc/explsup.html
Dahn, C. C., et al. 2002, AJ, 124, 1170
Deacon, N. R., Hambly, N. C., & Cooke, J. A. 2005, A&A, 435, 363
Dehnen, W., & Binney, J. J. 1998, MNRAS, 298, 387
Delfosse, X., et al. 1997, A&A, 327, L25
Filippenko, A. V. 1982, PASP, 94, 715
Geballe, T. R., et al. 2002, ApJ, 564, 466
Gizis, J. E. 2002, ApJ, 575, 484
Gizis, J. E., Monet, D. G., Reid, I. N., Kirkpatrick, J. D., Liebert, J., & Williams, R. 2000, AJ, 120, 1085
Gizis, J. E., Reid, I. N., Knapp, G. R., Liebert, J., Kirkpatrick, J. D., Koerner, D. W., & Burgasser, A. J. 2003, AJ, 125, 3302
Gizis, J., Shipman, H., & Harvin, J. 2005, ApJ, 630, L89
Goldman, B., et al. 1999, A&A, 351, L5
Golimowski, D. A., et al. 2004, AJ, 127, 3516
Goto, M., et al. 2002, ApJ, 567, L59
Hambly, N. C., Davenhall, A. C., Irwin, M. J., & MacGillivray, H. T. 2001a, MNRAS, 326, 1315
Hambly, N. C., Henry, T. J., Subasavage, J. P., Brown, M. A., & Jao, W.-C. 2004, AJ, 128, 437
Hambly, N. C., Irwin, M. J., & MacGillivray, H. T. 2001b, MNRAS, 326, 1295
Hambly, N. C., et al. 2001c, MNRAS, 326, 1279
Hawley, S. L., Gizis, J. E., & Reid, I. N. 1996, AJ, 112, 2799
Hawley, S. L., et al. 2002, AJ, 123, 3409
Hayes, D. S. 1985, in IAU Symp. 111, Calibration of Fundamental Stellar Quantities, ed. D. S. Hayes, L. E. Pasinetti, & A. G. D. Philip (Dordrecht: Reidel), 225
Henry, T. J., Jao, W.-C., Subsavage, J. P., Beaulieu, T. D., Lanna, P. A., Costa, E., & Mendez, R. A. 2006, AJ, 132, 2360
Henry, T. J., Subasavage, J. P., Brown, M. A., Beaulieu, T. D., Jao, W.-C., & Hambly, N. C. 2004, AJ, 128, 2460
Jayawardhana, R., & Ivanov, V. D. 2006, Science, 313, 1279
Jones, H. R. A., & Tsuji, T. 1997, ApJ, 480, L39
Kendall, T. R., Delfosse, X., Martín, E. L., & Forveille, T. 2004, A&A, 416, L17
Kendall, T. R., Jones, H. R. A., Pinfield, D. J., Porkorny, R. S., Folkes, S., Weights, D., Jenkins, J. S., & Mauron, N. 2007, MNRAS, 374, 445
Kirkpatrick, J. D. 2005, ARA&A, 43, 195
Kirkpatrick, J. D., Barman, T. S., Burgasser, A. J., McGovern, M. R., McLean, I. S., Tinney, C. G., & Lowrance, P. J. 2006, ApJ, 639, 1120
Kirkpatrick, J. D., Reid, I. N., Liebert, J., Gizis, J. E., Burgasser, A. J., Monet, D. G., Dahn, C. C., Nelson, B., & Williams, R. J. 2000, AJ, 120, 447
Kirkpatrick, J. D., et al. 1999, ApJ, 519, 802
Knapp, G., et al. 2004, AJ, 127, 3553
Koerner, D. W., Kirkpatrick, J. D., McElwain, M. W., & Bonaventura, N. R. 1999, ApJ, 526, L25
Kurucz, R. L., & Bell, B. 1995, Kurucz CD-ROM 23, Atomic Line Data, (Cambridge: SAO)
Lane, B. F., Zapatero Osorio, M. R., Britton, M. C., Martín, E. L., & Kulkarni, S. R. 2001, ApJ, 560, 390
Leggett, S. K., Allard, F., Geballe, T., Hauschildt, P. H., & Schweitzer, A. 2001, ApJ, 548, 908
Liu, M. C., & Leggett, S. K. 2005, ApJ, 634, 616
Liu, M. C., Leggett, S. K., Golimowski, D. A., Chiu, K., Fan, X., Geballe, T. R., Schneider, D. P., & Brinkmann, J. 2006, ApJ, 647, 1393
Lodieu, N., Scholz, R.-D., McCaughrean, M. J., Ibata, R., Irwin, M., & Zinnecker, H. 2005, A&A, 440, 1061
Luhman, K. L. 2004, ApJ, 614, 398
Mamajek, E. E. 2005, ApJ, 634, 1385
Martín, E. L., Brandner, W., Bouy, H., Basri, G., Davis, J., Deshpande, R., & Montgomery, M. 2006, A&A, 456, 253
McCaughrean, M. J., Close, L. M., Scholz, R.-D., Lenzen, R., Biller, B., Brandner, W., Hartung, M., & Lodieu, N. 2004, A&A, 413, 1029
McElwain, M. W., & Burgasser, A. J. 2006, AJ, 132, 2074
McGovern, M. R. 2005, Ph.D. thesis, Univ. California, Los Angeles
McGovern, M. R., Kirkpatrick, J. D., McLean, I. S., Burgasser, A. J., Prato, L., & Lowrance, P. J. 2004, ApJ, 600, 1020
McLean, I. S., McGovern, M. R., Burgasser, A. J., Kirkpatrick, J. D., Prato, L., & Kim, S. 2003, ApJ, 596, 561
Mohanty, S., & Basri, G. 2003, ApJ, 583, 451
Mohanty, S., Basri, G., Shu, F., Allard, F., & Chabrier, G. 2002, ApJ, 571, 469
Mohanty, S., Jayawardhana, R., & Barrado y Navascués, D. 2003, ApJ, 593, L109
Mohanty, S., Jayawardhana, R., Huélamo, N, & Mamajek, E. 2007, ApJ, 657, 1064
Morgan, W. W., Keenan, P. C., & Kellman, E. 1943, An Atlas of Stellar Spectra, with an Outline of Spectral Classification (Chicago: Univ. Chicago Press)

Mountain, C. M., Selby, M. J., Leggett, S. K., Blackwell, D. E., & Petford, A. D. 1985, A&A, 151, 399
Mugrauer, M., & Neuhäuser, R. 2005, Astron. Nachr., 326, 701
Nakajima, T., Oppenheimer, B. R., Kulkarni, S. R., Golimowski, D. A., Matthews, K., & Durrance, S. T. 1995, Nature, 378, 463
Nakajima, T., Tsuji, T., & Yanagisawa, K. 2004, ApJ, 607, 499
Potter, D., Martín, E. L., Cushing, M. C., Baudoz, P., Brandner, W., Guyon, O., & Neuhäuser, R. 2002, ApJ, 567, L133
Rayner, J. T., Toomey, D. W., Onaka, P. M., Denault, A. J., Stahlberger, W. E., Vacca, W. D., Cushing, M. C., & Wang, S. 2003, PASP, 115, 362
Rebolo, R., Martín, E. L., & Magazzu, A. 1992, ApJ, 389, L83
Rebolo, R., Zapatero Osorio, M. R., Madruga, S., Béjar, V. J. S., Arribas, S., & Licandro, J. 1998, Science, 282, 1309
Reid, I. N., Burgasser, A. J., Cruz, K., Kirkpatrick, J. D., & Gizis, J. E. 2001a, AJ, 121, 1710
Reid, I. N., Gizis, J. E., Kirkpatrick, J. D., & Koerner, D. 2001b, AJ, 121, 489
Reid, I. N., Lewitus, E., Allen, P. R., Cruz, K. L., & Burgasser, A. J. 2006, AJ, 132, 891
Reipurth, B., & Clarke, C. 2001, AJ, 122, 432
Roe, H. G. 2002, PASP, 114, 450
Ruiz, M. T., Leggett, S. K., & Allard, F. 1997, ApJ, 491, L107
Scholz, R.-D., McCaughrean, M. J., Lodieu, N., & Kuhlbrodt, B. 2003, A&A, 398, L29
Scholz, R.-D., & Meusinger, H. 2002, MNRAS, 336, L49
Schubert, G., & Walterscheid, R. L. 2000, in Allen's Astrophysical Quantities, ed. A. N. Cox (4th ed.; New York: AIP), 239
Siegler, N., Close, L. M., Cruz, K. L., Martín, E. L., & Reid, I. N. 2005, ApJ, 621, 1023
Simons, D. A., & Tokunaga, A. T. 2002, PASP, 114, 169
Skrutskie, M. F., et al. 2006, AJ, 131, 1163
Stassun, K., Mathieu, R. D., Vaz, L. P. R., Valenti, J. A., & Gomez, Y. 2006, Nature, 440, 311
Stephens, D. C. 2001, Ph.D. thesis, New Mexico State Univ.
———. 2003, in IAU Symp. 211, Brown Dwarfs, ed. E. Martín (San Francisco: ASP), 355
Testi, L., et al. 2001, ApJ, 552, L147
Tinney, C. G., Burgasser, A. J., & Kirkpatrick, J. D. 2003, AJ, 126, 975
Tokunaga, A. T., & Kobayashi, N. 1999, AJ, 117, 1010
Tokunaga, A. T., Simons, D. A., & Vacca, W. D. 2002, PASP, 114, 180
Tsuji, T., Ohnaka, K., & Aoki, W. 1996, A&A, 305, L1
Vacca, W. D., Cushing, M. C., & Rayner, J. T. 2003, PASP, 115, 389
Vrba, F. J., et al. 2004, AJ, 127, 2948
West, A. A., et al. 2004, AJ, 128, 426
Wilson, J. C., et al. 2001, AJ, 122, 1989
Zapatero Osorio, M. R., Lane, B. F., Pavlenko, Ya., Martín, E. L., Britton, M., & Kulkarni, S. R. 2004, ApJ, 615, 958